

tially shifted by about 60 pc meaning that the site of the most recent star formation is not located at the peak of the continuum. The same is detected by Izotov et al. (1997) in the optical but, in this case, the spatial shift is larger and about 200 pc. We interpret this as due to the larger contribution from the ionised gas to the NIR continuum than to the optical one, but it could also be partly an effect of extinction.

The L image, observed at the VLT with 0.5" seeing, reveals a very compact source at the position of the SSC 1+2. It is difficult to compare the location of this object with respect to the spectral profiles due to the lack of a reference point in the latter but, on the basis of this observation and the extinction derived at different wavelengths, we can envision the following picture.

Star formation occurs in a heavily obscured central core that contributes most of the IR emission. This core lies behind a dust-free region that instead emits the bulk of the optical radiation observed. The central burst produced a number of supernovae that polluted the interstellar medium with dust. Assuming that all the H α flux observed

is generated in the external shell and using standard line ratios we derive that the outer region contributes 50% of Br γ and only 25% of Br α . In other words, 75% of the star formation in SBS 0335-052 is only observable at 4 μ m! (see Hunt, Vanzi & Thuan 2001 for details). These results open a new view on SBS 0335-052 and possibly on star formation at high redshift. If the hidden star formation in SBS 0335052 is typical of young galaxies at high redshifts, then the cosmic star formation rate as derived from UV-optical observations would be underestimated by a factor 2–3. ISO surveys of distant galaxies (Flores et al. 1999) suggest that this is the case.

References

- Aloisi, A., Tosi, M., Greggio, L. 1999, *AJ*, **118**, 302.
 Flores H., Hammer F., Thuan T.X., Cesarsky C. et al. 1999, *ApJ* **517**, 148.
 Frogel J. 1985, *ApJ* **298**, 528.
 Hunt L.K., Vanzi L., & Thuan T.X. 2001, *A&A*, submitted.
 Izotov Y.I., Thuan T.X. 1998, *ApJ* **500**, 188.
 Izotov Y.I., Thuan T.X. 1999, *ApJ* **511**, 639.

- Izotov Y.I., Lipovetsky V.A., Chaffee F.H. et al 1997, *ApJ* **476**, 698.
 Leitherer C., Schaerer D., Goldader J.D. et al. 1999, *ApJS* **123**, 3.
 Kniazev A.Y., Pustilnik S.A., Masegosa J., Marquez I. et al. 2000, *A&A* **357**, 101.
 Kunth & Östlin 2000, *A&A Rev.* **10**, 1.
 Melnick J., Heydari-Malayeri M., Leisy P. 1992, *A&A* **253**, 16.
 Östlin, G. 2000, *ApJ* **535**, L99.
 Rieke G.H., Lebofsky M.J., Walker C.E. 1988, *ApJ* **325**, 687.
 Rieke G.H., Loken K., Rieke M.J., Tamblyn P. 1993 *ApJ* **412**, 111.
 Sauvage M., Thuan T.X., Lagage P.O. 1997, *A&A* **325**, 98.
 Steidel C.C., Gialalisco M., Pettini M., Dickinson M., Adelberger K.L. 1996, *ApJ* **462**, L17.
 Taylor C.L., Kobulnicky, H.A., Skillman E.D. 1998 *AJ*, **116**, 2746.
 Taylor C.L., Klein U. 2001, *A&A* **366**, 811.
 Thuan T.X., Izotov Y.I., Lipovetsky V.A. 1997, *ApJ* **477**, 661.
 Thuan T.X., Sauvage M., Madden S. 1999, *ApJ* **516**, 783.
 Thuan T.X., Lipovetsky, V.A., Martin J.M., Pustilnik S.A. 1999 *A&AS* **139**, 1.
 Todini P., Ferrara A. 2001, *MNRAS*, submitted.
 van Zee L. 2000, *ApJ* **543**, L31.
 Vanzi L., Rieke R.H., Martin C.L., Shields J.C. 1996, *ApJ* **466**, 150.
 Vanzi L., Hunt L.K., Thuan T.X., Izotov Y.I. 2000, *A&A* **363**, 493.

Eigenvector 1: An H-R Diagram for AGN?

J. W. SULENTIC¹, M. CALVAN², P. MARZIAN²

¹Department of Physics and Astronomy, University of Alabama, Tuscaloosa, AL, USA

²Osservatorio Astronomico di Padova, Padova, Italy

Abstract

Observations with 1.5-m-class ESO telescopes have contributed significantly to a much clearer understanding of the phenomenology of Active Galactic Nuclei (AGN) that has emerged over the past seven years. Long-slit spectra of good resolution and high s/n enable us to accurately measure emission-line parameters for a significant number of AGN. Combined with soft X-ray and UV line measures from Hubble Space Telescope, the data reveal a parameter space that distinguishes between the diverse classes of AGN and organises them in a way that promises to redefine the input to physical models. We suggest that this Eigenvector 1 (E1) parameter space may be as close as we will ever come to finding an H-R diagram for quasars. Several arguments suggest that the ratio of AGN luminosity to black hole mass ($L/M \propto$ accretion rate) convolved with the effects of source orientation drives the principal E1 correlation. While L/M sustains, in a sense, the H-R analogy beyond phenomenology, the

role of orientation reflects the greater complexity inherent in the lack of spherical symmetry for AGN.

1. Introduction

The H-R Diagram is well known as the most fundamental correlation space for stars. A plot of surface temperature vs. luminosity effectively discriminates between the diversity of normal and "abnormal" stellar types. Main-sequence stars show a strong correlation in the space while stars in other evolutionary stages are identified by their different domain space occupation. The fact that a 2-D correlation space is so effective reflects the simplicity of the law of hydrostatic equilibrium that governs stellar structure. Thus the principal driver of the correlation space is stellar mass. It is possible that after less than 50 years of study we might see a similar correlation space on the horizon for Active Galactic Nuclei (AGN). ESO spectroscopic observations have made a significant contribution to the work that has led to the Eigenvector 1 concept. The fundamental parameters of

an AGN correlation space might be expected to be more numerous than those for a stellar diagram because we are observing a combination of primary continuum and secondary line and continuum emission components in a structure with complex geometry. In fact, the 2-D optical (for low z quasars) parameter plane reveals much of the correlation power. In its present evolution our 4-D Eigenvector 1 correlation space shows a phenomenological discrimination in several ways comparable with that of the H-R diagram for stars. The veracity and implications of that statement will likely be the subject of much research in the next decades.

A defining characteristic of AGN involves the presence of broad emission lines (usually FWHM H $\beta \geq 10^3$ km/s). This definition encompasses Seyfert 1 nuclei, QSO's, broad line radio galaxies and quasars. BLLACs (in low continuum phase) and Seyfert 2 nuclei (in polarised light) also sometimes show broad lines. Although the first AGN (quasars) were discovered because of their radio-loudness, it is now known that the bulk of AGN are radio-quiet.

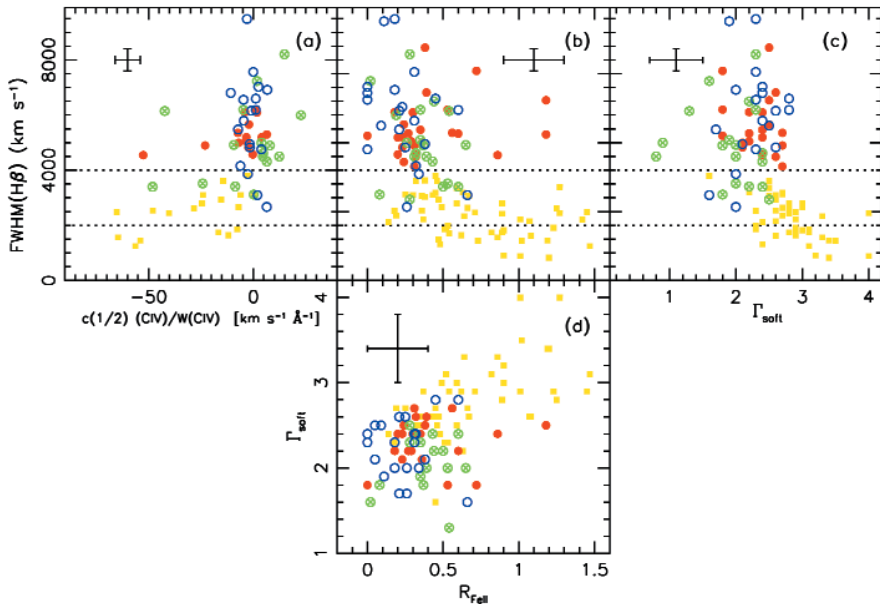


Figure 1: Principal correlates of the E1 parameter space. The central panel (b) shows the optical E1 plane: $FWHM(H\beta)$ vs. RFE. RQ Population A sources (yellow squares), RQ population B (red circles), core-dominated RL (green circles) and lobe-dominated RL (blue open circles). Other E1 panels shown are: (a) $FWHM(H\beta)$ vs $CIV\lambda.1549$ shift normalised by rest frame equivalent width; (c) $FWHM(H\beta)$ vs Γ_{soft} and (d) Γ_{soft} vs. RFE. Horizontal lines mark the approximate FWHM upper limits for NLSy1 (2000 km/s) and RQ population A (4000 km/s) sources.

Radio-loudness in this context involves sources with a radio continuum flux $SR > 100$ times larger than an optical continuum value (see e.g. Kellermann et al. 1989). Various unification schemes have been proposed to unite all of the AGN phenomenology under the umbrella of a model that assumes: (1) the ultimate energy source as gravitational accretion onto a supermassive black hole and (2) an obscuring torus that prevents us from observing broad lines in sources inclined within $\approx 45^\circ$ of edge-on to our line of sight.

2. Eigenvector 1 Parameters

We currently define Eigenvector 1 in terms of four parameters:

1. Full width half maximum of the low ionisation broad lines (LIL: $H\beta$ is the current favourite because it is reasonably strong, not impossibly contaminated by other lines and yields optical measures for sources out to a redshift of $z \sim 1.0$) ($FWHM(H\beta)$).

2. The equivalent width (EW) ratio of the optical FeII emission (usually the FeII Ångstrom 4570 blend) and broad line $H\beta$ (RFE).

3. The soft X-ray photon index which is thought to measure a thermal emission feature seen in the 0.1–2.4 keV range for many AGN (Γ_{soft}).

4. The FWHM centroid velocity shift of the high ionisation broad lines ($CIV\lambda.1549$ is the easiest to measure) ($C(1/2)_{CIV}$).

We focus on the first two (optical) parameters and indeed the H-R analogy is obvious there. The optical parameters first appeared in a correlation

analysis of LIL emission-line data for PG bright quasars (Boroson & Green 1992). Our ESO observations helped to double the number of sources with such measures. Γ_{soft} measures come from numerous ROSAT observations (e.g. Wang et al. 1996; Brinkmann et al. 1997) while $C(1/2)_{CIV}$ emerged from the first large sample comparison of HIL and LIL in the same sources (Sulentic et al. 1995b; Marziani et al. 1996). Figure 1 shows the four most studied planes of E1. We plot data for sources with spectra having (in most cases) $s/n > 30$ (continuum near $H\beta$) and resolution better than 10 \AA (see Sulentic et al. 2000a,b for details). We find that addition of data with lower resolution and s/n quickly blurs all important structure and correlation in E1. There is no substitute for high s/n and moderate/high-resolution spectra. Many, of these sources ($n = 128$) have matching X-ray and UV data ($n = 76$). At this point our sample is mixed with major data components from the reasonably complete PG bright quasar sample and a heterogeneous sample of sources with HST archival UV spectra. The latter element results in an over-representation of radio-loud (RL) sources. The results so far suggest that E1 organises the AGN phenomenology better than any previous result.

3. Domain Occupation and Correlation in Eigenvector 1

Narrow-line Seyfert 1 (NLSy1) galaxies occupy one parameter domain extremum in E1. They show: (a) the narrowest broad line (down to 800 km/s)

LIL profiles; (b) largest RFE; (c) strongest soft X-ray excess and (d) a systematic CIV blueshift with values as large as 4–5000 km/s. At the opposite extremum we find steep spectrum (lobe dominated) radio-loud sources with: (a) the broadest LIL profiles (up to $FWHM = 23,000 \text{ km/s}$); (b) smallest RFE, (c) no soft X-ray excess and (d) a stochastic distribution of red and blue CIV centroid shifts (a mean near 0 km/s). Aside from the difference in domain space occupation for RL and RQ sources, we find that both radio and optical continuum luminosity appear to be uncorrelated with E1 parameters. We tentatively identify two radio-quiet populations in Figure 1: “Pure RQ” Population A (yellow) with $FWHM(H\beta) \leq 4000 \text{ km/s}$ and Population B (red) with the same domain occupation as the majority of RL sources (flat spectrum – green and steep spectrum – blue). The few RQ sources in the “forbidden zone” of the optical E1 plane (large FWHM and RFE) generally show broad absorption lines, excess IR emission and ultra strong FeII emission – this may be the domain of type 2 (obscured) quasars. Population A sources show significant intercorrelation between all parameters (a “main sequence”?) which breaks down in the RL/RQ population B domain. It is not yet possible to say if this reflects larger uncertainties for measurements of the broader line sources.

Figure 2 shows ESO spectra for two RQ sources (population A NLSy1 Ton 28 and population B RQ Seyfert 1 NGC 3783) that illustrate well the extreme differences found between AGN in the RQ population A and B domains. The ESO data alone show the full optical phenomenological differences revealed by E1. The days are clearly gone when one can say that all quasars look alike spectroscopically! Figure 3 shows the matching $CIV\lambda.1549$ line profiles obtained through ESO-ST-ECF. We also show our ESO spectrum of Pictor A which further emphasises the line profile differences across E1. This RL source is typical of the most extreme lobe-dominated RL sources that show the broadest observed LIL Balmer lines. It is a true opposite extreme from Ton 28 in all the E1 parameters. Table 1 provides a summary of average parameter values across E1.

4. Towards a Physical Interpretation

Attempts to model E1 have so far focused on the optical plane where the ESO observations have played an important role. This is also where the “H-R” analogy is most compelling. It is the plot of line width versus the intensity ratio of two different atomic species that can be easily measured for a large number of quasars. Absorption line widths and line intensity ratios vary

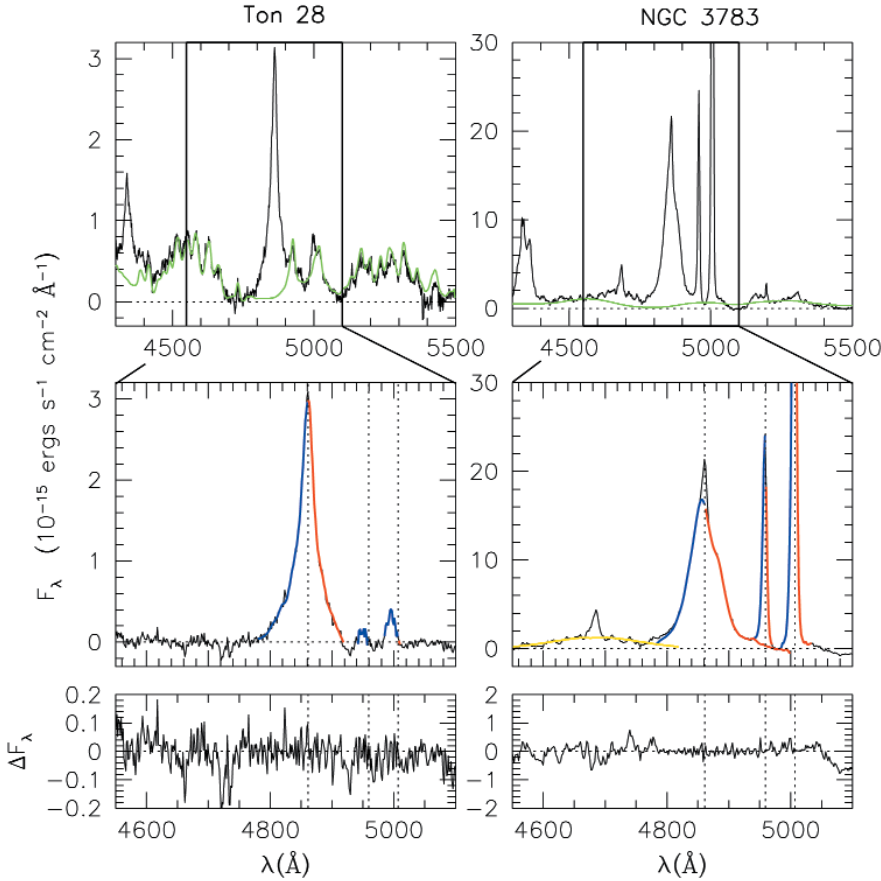
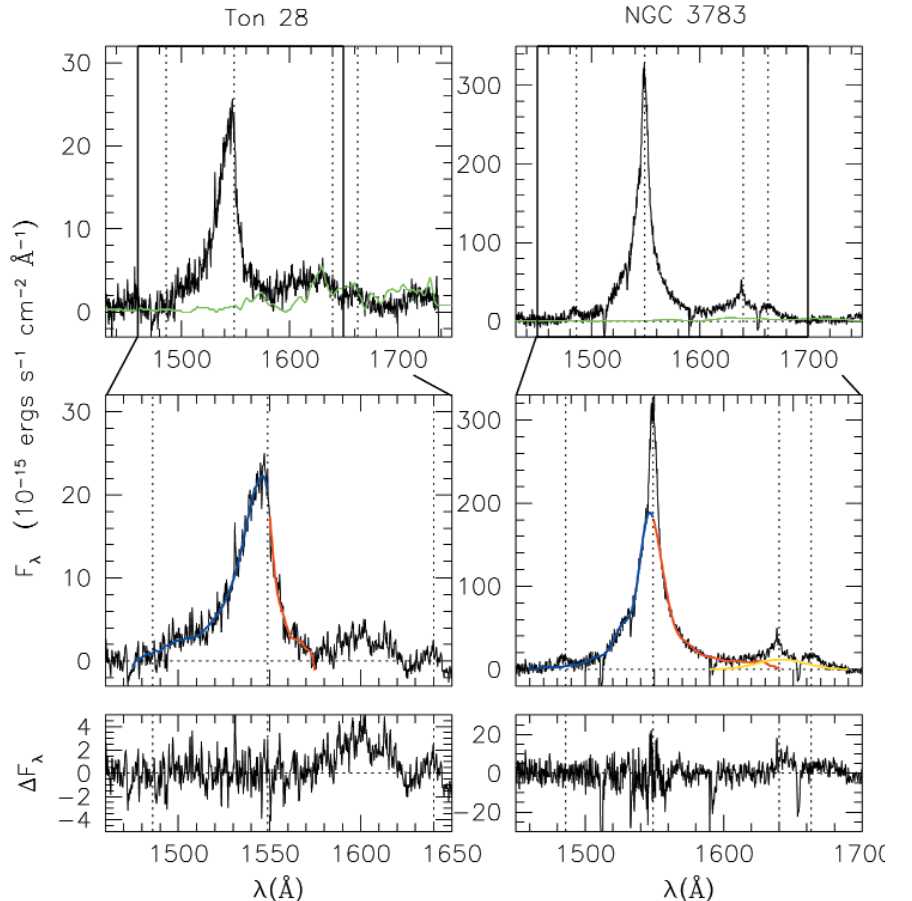


Figure 2: Comparison of ESO spectra for the $H\beta$ region of a NLSy1 Population A source (Ton 28) and a RQ Population B source (NGC 3783). Upper panels show the continuum subtracted, flux-calibrated spectra. We superimpose the adopted FeII emission model (green). The middle panels zoom the wavelength range around $H\beta$ in order to better show the line profile. The vertical dotted lines indicate the rest-frame wavelengths of $H\beta$ and the $[OIII]\lambda\lambda 4959, 5007$ lines. Blueward and redward wings of the broad component of $H\beta$ and the $[OIII]$ lines are traced in red and blue to better emphasise profile asymmetries and shifts. The thick yellow line shows a gaussian fit to a very broad $H\beta$ emission component. The lower panels show the residual spectrum after subtraction of continuum, FeII, and all identified lines.

across the H-R diagram and are central to our understanding of stellar physics. In fact, the optical plane of E1 illustrates well the role of the principal physical drivers in E1. The X-ray and CIV $\lambda 1549$ measures provide additional and strong support for our interpretation with the latter, our best hope for decoupling the effects of source orientation. Independent studies which interpret the soft X-ray excess as a thermal feature and the UV CIV blueshift as a wind or outflow motivate the suggestion that they are directly related to an accretion disk surrounding the central black hole. Thus we begin our inter-

Figure 3: Comparison of ST-ECF archival data for the CIV $\lambda 1549$ spectral regions in Ton 28 and NGC 3783. Spectra are displayed in the same manner as for $H\beta$ (Figure 2). Note the large CIV profile blueshift in NLSy1 Ton 28.



pretation of the optical plane with the assumption that NLSy1 sources are the class of AGN with the highest accretion rate.

A long-standing problem for BLR models has involved explaining the strength and dispersion of FeII emission observed in AGN. The optical FeII lines arise from collisional excitation, and therefore assumptions of high density and large column density are required to model them. The presence of strong FeII emission, especially in population A sources, makes an accretion disk origin for FeII production an attractive possibility. A medium that favours strong FeII emission may, at the same time, collisionally suppress $H\beta$ emission. Perhaps this combination explains why the EW ratio RFE is so extreme in NLSy1 and shows such a large dynamic range across E1. At the same time FWHM ($H\beta$) in such a scenario is likely to be orientation sensitive. The narrow FWHM measures found for many NLSy1 argue that at least some of them are seen near face-on (this argument is supported by the short time-scale high amplitude X-ray variability seen in some NLSy1). We have developed a model where we express the E1 parameters and the model physics in terms of the AGN luminosity to black hole mass ratio ($L/M \propto$ Eddington ratio = the dimensionless accretion rate). This allows us to predict the expected values of the optical E1 parameters for a typical black-hole mass convolved

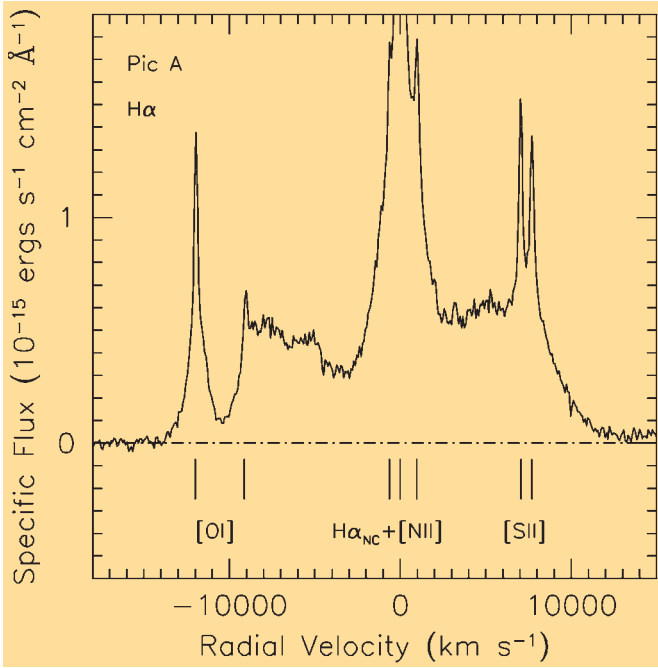


Figure 4: ESO spectrum of the complex and ultra-broad $H\alpha$ profile of Pictor A. This records its appearance on December 18, 1993. The source was single peaked and much narrower 5–10 years before this date.

with a range of source orientation from near face-on (10°) to near torus obscured (40°). In Figure 5 our model fits are superimposed on the optical E1 plane and appear to predict the principal zone of occupation/correlation quite well. The analogy to the “main sequence” is apparent except that L/M is convolved with source orientation while M is an orientation independent physical driver of the main sequence. In this interpretation NLSy1 sources with the hottest disks and strong wind outflows suggest an analogy with the hottest main sequence OB stars.

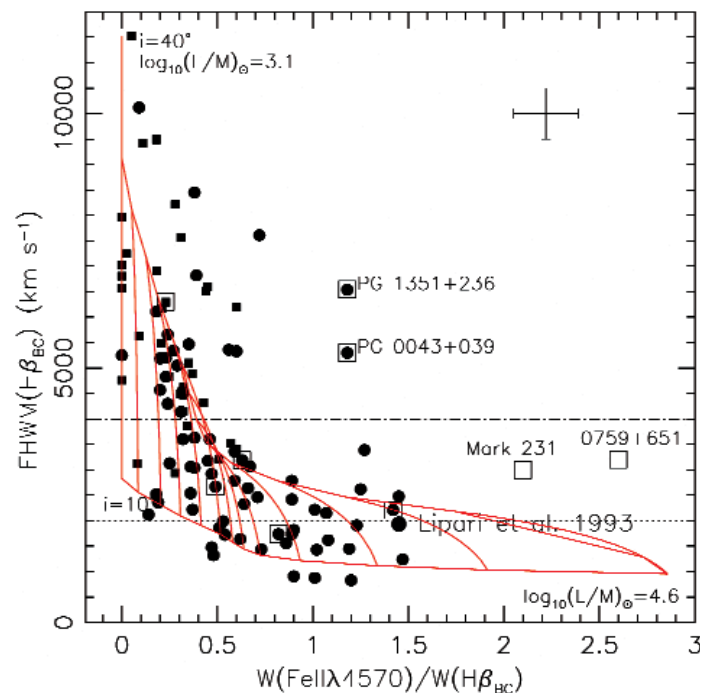
Our model is focused on the population ARQ sources and suggests that E1 is measuring several accretion disk properties that reflect a high accretion rate. Ironically the RL sources that were argued, just a few years ago, to be the best candidates for disk line emission may be the lowest accreting AGN. We are exploring the possibility that RL and RQ population B sources lie below a critical accretion threshold where the disk could be optically thin, transient or nonexistent. The line profile of Pictor A (Figure 4) has indeed shown dramatic changes over the past 15 years (Sulentic et al. 1995a). Several properties of these low-accreting sources are consistent with line production in a bi-conical outflow.

5. Conclusion

How is it possible that potentially fundamental results about AGN could emerge from observations with telescopes with small/moderate aperture? The first response is that a significant number of quasars are brighter than $V = 16.0$ so that excellent spectra can be obtained with investments of 0.5–

2.0 hours. The second is that very few people are now working on spectroscopy of the broad emission lines. The reasons for the paucity of researchers are complex but one of them is that some people moved away from the field because of a sense of frustration about the diversity of AGN spectra and the very few strong line related correlations that had been found. Eigenvector 1 is likely to change that. Obviously we are overstating the E1 – HR analogy here, and a lot of work still remains to be done on the interpretation – as well as on testing whether the same scenario may still be valid at higher redshift and source luminosity. But if the domain occupation and correlation in E1 proves to be robust

Figure 5: Model grid of the expected distribution of RQ population A sources superimposed on the E1 optical plane. Model assumes that L/M (\propto dimensionless accretion rate) is the principal physical driver (convolved with effects of source orientation). Grid is shown in steps of $L/M = 0.1$ over an inclination range of 10 – 40 degrees for a $\log M = 8.0$ black hole. BAL quasars are boxed symbols.



with larger and high-quality data samples then the analogy will have been justified.

7. Acknowledgements

We are indebted to several colleagues who took part in the work involving ESO data and who helped us to gain access to northern-hemisphere observing time (D. Dultzin-Hacyan, T. Zwitter, M. Moles). We also acknowledge financial support from the Italian Ministry of University and Scientific and Technological Research (MURST) through grants Cofin 98 – 02 – 32 and Cofin 00 – 02 – 004. J.S. acknowledges with gratitude hospitality and support from Osservatorio Astronomico di Padova, Brera and Merate where parts of the work were carried out.

References

- Brinkmann, W., Yuan, W., and Siebert, J. 1997, *A&A*, **319**, 413.
- Boroson, T. A., and Green, R. F. 1992, *ApJS*, **80**, 109 (BG92).
- Kellermann K. I., Sramek R., Schmidt M., Shaffer D. B. and Green R. 1989, *AJ*, **98**, 1195.
- Marziani, P., Sulentic, J. W., Dultzin-Hacyan, D., Calvani, M., & Moles, M. 1996, *ApJS*, **104**, 37.
- Marziani, P., Sulentic, J. W., Zwitter T., Dultzin-Hacyan D., and Calvani, M., 2001, *ApJ*, in press.
- Sulentic, J. W., Marziani, P., Zwitter, T. and Calvani, M., 1995a, *ApJ*, **438**, 1.
- Sulentic, J. W., Marziani, P. Dultzin-Hacyan, D., Calvani, M. and Moles, M., 1995b, *ApJ*, **445**, 85.
- Sulentic, J. W., Marziani, P. and Dultzin-Hacyan, D. 2000a, *ARA&A*, **38**, 521.
- Sulentic, J. W., Zwitter, T., Marziani, P., and Dultzin-Hacyan, D. 2000b, *ApJL*, **536**, L5.
- Wang T, Brinkmann W., Bergeron J. 1996, *A&A* **309**, 81–86.